Langmuir
Article
pubs.acs.org/Langmuir

Brightly Phosphorescent, Environmentally Responsive Hydrogels Containing a Water-Soluble Three-Coordinate Gold(I) Complex

Sreekar Marpu,[†] Zhibing Hu,*[,‡,†] and Mohammad A. Omary*[,§,†]

[†]*Departments of Material Science and Engineering,* [‡]*Physics, and* [§]*Chemistry, University of North Texas, Denton, Texas 76203*

Received April 22, 2010. Revised Manuscript Received July 21, 2010

Stimuli-responsive phosphorescent hydrogel microspheres have been synthesized by incorporating a water-soluble phosphorescent Au(I) complex, $Na_8[Au(TPPTS)_3]$, TPPTS = tris(3,3′,3″-trisulfonatophenyl)phosphine, into the polymer network of poly(*N*-isopropylacrylamide) (PNIPAM). Remarkable sensitization of the Au-centered emission takes place in the resulting phosphorescent hydrogels (*by up to 2 orders of magnitude!*) compared to that of the gold complex alone in pure water. Results of pH- and temperature-dependent luminescence titrations show that the sensitization is further magnified at physiological conditions, which is desirable for biomedical applications that will include bioimaging and drug delivery. The physical properties of PNIPAM microgels are not negatively impacted by the presence of the gold luminophore, as the colloidal crystallinity and phase transition properties remain intact. Phosphorescent microspheres have been further cross-linked by covalently bonding to neighboring particles, leading to brightly phosphorescent/high-water-content crystalline hydrogel networks with more stable crystallinity vs microgel soft crystals. These gel networks exhibit the same green phosphorescence seen in the hydrogel microspheres and pure $Na_8[Au(TPPTS)_3]$ aqueous solutions with a broad unstructured profile and peak maximum at ∼525 nm. Dehydration leads to further emission sensitization and gradual blue shifts that can be fine-tuned to ultimately reach a turquoise emission at ∼490 nm in the freeze-dried form of the gel, corresponding to the emission of single crystals of $Na_8[Au(TPPTS)_3]$, in agreement with the photoinduced Jahn−Teller distorted excited state model we reported earlier. Remarkable sensitivity to temperature and pH takes place in the emission enhancement with particularly favorable results at physiological conditions. The work herein represents a unique example of a stimulus-responsive phosphorescent hydrogel from a transition metal-based as opposed to lanthanide-based phosphor in an aqueous medium.

1. Introduction

Hydrogels are composed of hydrophilic organic polymer networks cross-linked physically or chemically.[1] Some hydrogels exhibit stimulus-sensitive behavior that leads to undergoing conformational changes in response to various external variables such as pH,[2] temperature,[3] electric,[4] magnetic,[5] and/or optical[6] stimuli. Such materials have been called "smart" or "intelligent" hydrogels[7] because the aforementioned behavior allows them to be useful for various biomedical applications such as site-specific and controlled drug delivery,[8,9] tunable optics and biosensors,[10] encapsulation of cells,[11] molecular imaging,[12] immobilization of enzymes and cells,[13] protein assays,[14] separation and wastewater remediation,[15] and *in vitro* tissue formation.[16] Poly(*N*-isopropylacrylamide) (PNIPAM) represents the most extensively studied stimulus-sensitive polymer hydrogel material.[7,17] Studies on hydrogels already covered a broad domain in materials science; little attention has been paid, however, to hydrogels as hosts for versatile molecular luminophores. Though studies of ligand−lanthanide luminescent molecules in connection with hydrogels as host matrixes are known,[18] similar studies using a transition-metal-based luminescent complex are yet unexplored, perhaps due to limited pursuit of water-soluble and -stable systems that exhibit sufficiently bright phosphorescence at physiological conditions.

*To whom correspondence should be addressed. E-mail: omary@unt.edu (M.A.O.); zbhu@unt.edu (Z.H.).

(1) Nayak, S.; Lyon, A. L. *Angew. Chem., Int. Ed.* **2005**, *44*, 7686.
(2) Siegel, R. A.; Firestone, B. A. *Macromolecules*. **1988**, *21*, 3254.
(3) (a) Hirotsu, S.; Hirokawa, Y.; Tanaka, T. *J. Chem. Phys.* **1987**, *87*, 1392. (b) Wang, J.; Gan, D.; Lyon, A. L.; El-Sayed, M. A. *J. Am. Chem. Soc*. **2001**, *123*, 11284. (c) Suzuki, D.; Tsuji, S.; Kawaguchi, H. *J. Am. Chem. Soc*. **2007**, *129*, 8088. (d) Keerl, M.; Pedersen, J. S.; Richtering, W. *J. Am. Chem. Soc*. **2009**, *131*, 3093.
(4) (a) Kwon, I. C.; Bae, H. Y.; Kim, W. S. *Nature* **1991**, *354*, 291. (b) Osada, Y.; Okuzaki, H.; Hori, H. *Nature* **1992**, *355*, 242.
(5) (a) Chen, J.; Yang, L.; Ding, G.; Lie, J.; Huang, G. *Macromol. Symp*. **2005**, *225*, 71. (b) Kondo, A.; Fukuda, H. *J. Ferment. Bioeng*. **1997**, *84*, 337.
(6) (a) Jones, C. D.; Serpe, M. J.; Schroeder, L.; Lyon, L. A. *J. Am. Chem. Soc*. **2003**, *125*, 5292. (b) Gorelikov, I.; Field, L. M.; Kumacheva, E. *J. Am. Chem. Soc*. **2004**, *126*, 15938. (c) Garcia, A.; Marquez, M.; Cai, T.; Rosario, R.; Hu, Z. B.; Gust, D.; Hayes, M.; Vail, S. A.; Park, C. *Langmuir* **2007**, *23*, 224. (d) Pelton, R. *Adv. Colloid Interface Sci*. **2000**, *85*, 1.
(7) For reviews, see: (a) Peppas, N. A. *Hydrogels in Medicine and Pharmacy*; CRC Press: Boca Raton, FL, 1986. (b) Hoffman, A. S. *Adv. Drug Delivery Rev*. **2002**, *43*, 3.
(8) (a) Hu, Z.; Gao, J. *Langmuir* **2002**, *18*, 1360. (b) Gao, J.; Frisken, B. *Langmuir* **2005**, *21*, 545. (c) Hu, Z.; Huang, G. *Angew. Chem., Int. Ed*. **2003**, *42*, 4799. (d) Xia, X.; Hu, Z.; Marquez, M. *J. Controlled Release* **2005**, *103*, 21. (e) Tang, S. J.; Hu, Z. B.; Zhou, B.; Cheng, Z. D.; Wu, J. Z.; Marquez, M. *Macromolecules* **2007**, *40*, 9544.
(9) (a) Qui, Y.; Park, K. *Adv. Drug Delivery Rev*. **2001**, *53*, 321. (b) Bouhadir, H. K.; Alsberg, E.; Mooney, J. D. *Biomaterials* **2001**, *22*, 2625. (c) Moretto, A.; Tesolin, L.; Marsilio, F.; Berna, M.; Veronese, F. M. *IL FARMCO* **2004**, *59*, 1. (d) Huang, G.; Hu, Z.; John, V.; Ponder, B. C.; Moro, D. *J. Controlled Release* **2004**, *94*, 303. (e) Petrak, K. *Drug Discovery Today* **2005**, *23*/*24*, 1667.
(10) (a) Reese, C. E.; Mikhonin, A. V.; Kamenjicki, M.; Tikhonov, A.; Asher, S. A. *J. Am. Chem. Soc*. **2004**, *126*, 1493. (b) Kim, J.; Serpe, J. M.; Lyon, A. L. *J. Am. Chem. Soc*. **2004**, *126*, 9512.
(11) Mathew, W. H.; Salley, O. S.; Peterson, D. W.; Klein, D. M. *Biotechnol. Prog*. **1993**, *9*, 510.
(12) Apkarian, P. R.; Wright, R. E.; Seredyuk, A. V.; Eustis, S.; Lyon, A. L.; Conticello, P. V.; Menger, M. F. *Microsc. Microanal*. **2003**, *9*, 286.
(13) Ozkul, N. A.; Khare, A. R. *Adv. Drug Delivery Rev*. **1993**, *11*, 1.
(14) Kim, J.; Lyon, A. L.; Nayak, S. *J. Am. Chem. Soc*. **2005**, *127*, 9588.
(15) (a) Kiousis, R. D.; Smith, F. D.; Kofinas, P. *J . Appl. Polym. Sci*. **2001**, *80*, 2073. (b) Kofinas, P.; Kiousis, R. D. *Environ. Sci. Technol*. **2003**, *37*, 423.
(16) (a) Stile, A. R.; Burghardt, R. W.; Healy, K. E. *Macromolecules* **1999**, *32*, 7370. (b) Boelen, J. H. E.; Hooy-Corstjens, S. J. C.; Bulstra, k. S.; Koole, H. L.; Rhijn, W. L. *Biomaterials* **2005**, *26*, 6674. (c) Byrne, E. M.; Park, K.; Peppas, N. A. *Adv. Drug Delivery Rev*. **2002**, *54*, 149.
(17) Gao, J.; Frisken, J. B. *Langmuir*. **2003**, *19*, 5217.
(18) (a) Yan, B.; Xiang, Y.; Wang, Q.; Liu, Y. *J. Fluoresc*. **2006**, *16*, 723. (b) Huang, X.; Lu, T.; Chen, M.; Guo, X. *J. Polym. Res*. **2008**, *15*, 41. (c) McCoy, P. C. *Chem. Mater*. **2006**, *18*, 4336.

Given the quantum leap that phosphorescent transition-metal complexes have caused in photonic applications such as organic light-emitting diodes,[19] it is important to pursue applications that take advantage of their remarkable photophysical properties by seeking strategies that enable their introduction to biocompatible media such as hydrogels. The work herein represent our first effort to fill this gap (Patent Pending) by introducing the water-soluble phosphorescent transition metal compound $Na_8[Au(TPPTS)_3]$ into the polymer network of PNIPAM (Chart 1).

Phosphorescent hydrogels can enable experiments such as tracking diffusional processes, monitoring phase transformations of entangled biopolymers, and sensing environmental stimuli.[20] In their swollen state, hydrogels are usually transparent and colorless while in their collapsed state they become turbid. Advances in instrumentation technology have rendered luminescence spectroscopy a very versatile and powerful yet readily accessible tool for the characterization of polymers and hydrogel systems.[20] In order to track the gel swelling behavior or to monitor the location of gel particles in cells, fluorescent dyes or quantum dots are typically used so that the hydrogels are distinguished from the surrounding biological environment.[21] In this process, fluorescent labels have some disadvantages that include short nanosecond lifetimes that may coincide with any biological background emission (autofluorescence), self-quenching effects, high photobleaching, and weak fluorescence intensity at physiological pH.[22] Some of these disadvantages are predicted to be overcome by different emission enhancement mechanisms such as the enhancement in presence of either plasmonic colloidal metal nanoparticles[22b] or a micelle medium.[22e] Though there is considerable literature work on explaining the mechanism of metal colloid-based enhancement with different fluorophores,[22b,c] little is known about the exact mechanism of fluorescence enhancement mechanism in the presence of micelles. Fluorescence enhancement in the presence of a micelle medium is predicted to result from a combination of various factors that include enhanced stability or solubility of the fluorophore and/or decrease in nonradiative decay of the fluorophore in the presence of a micelle medium; however, a definitive mechanism about fluorescence or phosphorescence enhancement in the presence of a micelle or scattering polymeric colloidal medium is not well-documented.

There are few examples in the literature explaining the effect of PNIPAM or other polymer-based systems on the luminescent properties of lanthanide complexes. Work by Huang and co-workers[18b] detailed interactions of Tb(III) with PNIPAM-*co*-styrene microspheres. McCoy and co-workers reported the incorporation of Eu(III)-based complexes into methyl methacrylate:hydroxyethyl methacrylate (MMA:HEMA) hydrogels.[18c] The Wang group showed the formation of PNIPAM polymer chain incorporating a Tb(III) complex in the solid state, leading to emission enhancement of Tb(III) in PNIPAM/Tb(III) systems due to effective intramolecular energy transfer from the PNIPAM polymer chain to the Tb(III) centers.[18a] In this paper, we show that the phosphorescence of a three-coordinate gold(I) phosphor can be enhanced by more than an order of magnitude compared to the situation in a plain aqueous medium at different temperatures. While Raman scattering enhancement is well-documented for detection of small molecules at very low concentrations,[22d] the work herein paves the way to a wider scope of research by the simpler and more widely accessible method of steady-state photoluminescence spectroscopy to enable scattering-stimulated enhanced detection of molecules at very low concentrations. Thus, we demonstrate the loading of a highly stable water-soluble polyanionic three-coordinate gold(I) complex, $[Au(TPPTS)_3]^{8-}$, into stimulus-responsive PNIPAM hydrogel colloidal particles in aqueous medium without sacrificing the environmental sensitivity of the hydrogel while simultaneously sensitizing the Au-centered phosphorescence. The selection of three-coordinate Au(I) complexes as phosphors for this project is inspired by the work of Fackler, Assefa, and co-workers, who reported that some of these complexes can maintain their luminescence even in aqueous solution;[23] the work fits within the realm of our own interest in this class of complexes toward understanding their excited-state structure and the consequent impacts on photonic applications.[24]

Chart 1. Structures of the Gold Phosphor and Polymer Hydrogel Used

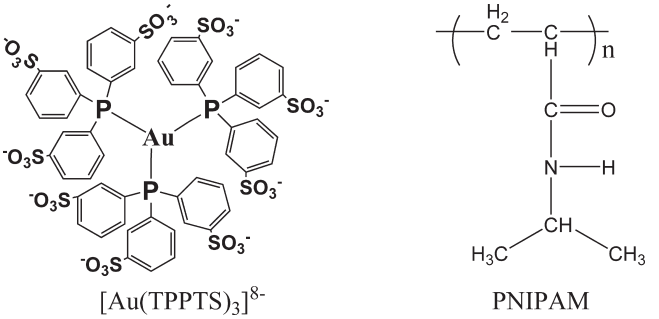

$[Au(TPPTS)_3]^{8-}$ PNIPAM

2. Materials and Methods

2.1. Materials. *N*-Isopropylacrylamide = "NIPA monomer" and *N,N′*-methylenebis(acrylamide) = "BIS" were purchased from Polysciences Inc. The Na_9TPPTS ligand and the chemicals needed for syntheses of different PNIPAM-based gels were purchased from Sigma-Aldrich and used as received. Millipore water was used as solvent for all experiments.

2.2. Syntheses of the Gold Phosphor. The phosphorescent gold compound $Na_8[Au(TPPTS)_3]$ was synthesized by adding 3 equiv of Na_9TPPTS to Au(tetrahydrothiophene)Cl, based on the procedure described in ref 23b. The purity of the complex was ascertained via ^{1}H and $^{31}P\{^1H\}$ NMR, IR, electronic absorption and emission, and time-resolved luminescence spectroscopic data compared to the literature (see Supporting Information).

2.3. Syntheses of PNIPAM Microgels. The hydrogel nanoparticles were made (Scheme 1) using the free radical precipitation polymerization method.[6d,8c] Thus, 3.8 g of the *N*-isopropylacrylamide monomer, 0.2 g of either allylamine or acrylic acid (for PNIPAM-*co*-allylamine or PNIPAM-*co*-acrylic acid, respectively),

(19) (a) D'Andrade, B. W.; Forrest, S. R. *Adv. Mater.* **2004**, *16*, 1585. (b) Reineke, S.; Lindner, F.; Schwartz, G.; Seidler, N.; Walzer, K.; Lüssem, B.; Leo, K. *Nature* **2009**, *459*, 234.

(20) Rangarajan, B.; Coons, L. S.; Scranton, A. B. *Biomaterials* **1996**, *17*, 649.

(21) (a) Wu, Z.; Gong, S.; Li, C.; Zhang, Z.; Huang, W.; Meng, L.; Lu, X.; He, Y. *Eur. Polym. J.* **2005**, *41*, 1985. (b) Gao, H.; Zhao, Y.; Fu, S.; Li, B.; Li, M. *Colloid Polym. Sci.* **2002**, *280*, 653. (c) Das, R. R.; Samal, S.; Choi, S. S.; Geckler, K. *Macromol. Rapid Commun.* **2001**, *22*, 850. (d) Gong, Y.; Gao, M.; Wang, D.; Mohwald, H. *Chem. Mater.* **2005**, *17*, 2648. (e) Li, J.; Hong, X.; Liu, Y.; Wang, Y.; Li, J. *Adv. Mater.* **2005**, *17*, 163.

(22) (a) Kam-Wing Lo, K.; Chun-Ming, D.; Chi-Keung, C. *Organometallics* **2001**, *20*, 4999. (b) Lakowicz, J. R. *Anal. Biochem.* **2001**, *298*, 1. (c) Wang, Y. H.; Zhou, J.; Zong, R. L.; Shi, S. K.; Wang, T.; Li, B. *Optoelectron. Lett.* **2006**, *2*, 0316. (d) Kneipp, K.; Wang, Y.; Kneipp, H.; Perelman, L. T.; Irving, I.; Dasari, R. R.; Feld, M. S. *Phys. Rev. Lett.* **1996**, *78*, 1667. (e) Takeuchi, T. *J. Chromatogr. A* **1997**, *780*, 219. (f) Sanz-Medel, A.; Alonso, J. I. G.; Gonzllez, E. B. *Anal. Chem.* **1985**, *57*, 1681. (g) Susumu, K.; Medintz, I. L.; Mattoussi, H. Colloidal quantum dots: synthesis, photophysical properties and biofunctionalization strategies. In *Inorganic Nanoprobes for Biological Sensing and Imaging*; Mattoussi, H., Cheon, J., House, A., Eds.; Artech House Publishers: Norwood, MA, 2008; Chapter 1, pp 1−26.

(23) (a) Forward, M. J.; Assefa, Z.; Fackler, J. P., Jr. *J. Am .Chem. Soc.* **1995**, *117*, 9103. (b) Assefa, Z.; Forward, M. J.; Grant, A. T.; Staples, J. R.; Hanson, E. B.; Fackler, J. P., Jr. *Inorg. Chim. Acta* **2003**, *352*, 31.

(24) (a) Sinha, P.; Wilson, A. K.; Omary, M. A. *J. Am. Chem. Soc.* **2005**, *127*, 12488. (b) Barakat, K. A.; Cundari, T. R.; Omary, M. A. *J. Am. Chem. Soc.* **2003**, *125*, 14228.

Scheme 1. Synthesis of PNIPAM-*co*-Allylamine, PNIPAM, and PNIPAM-*co*-Acrylic Acid Microgels

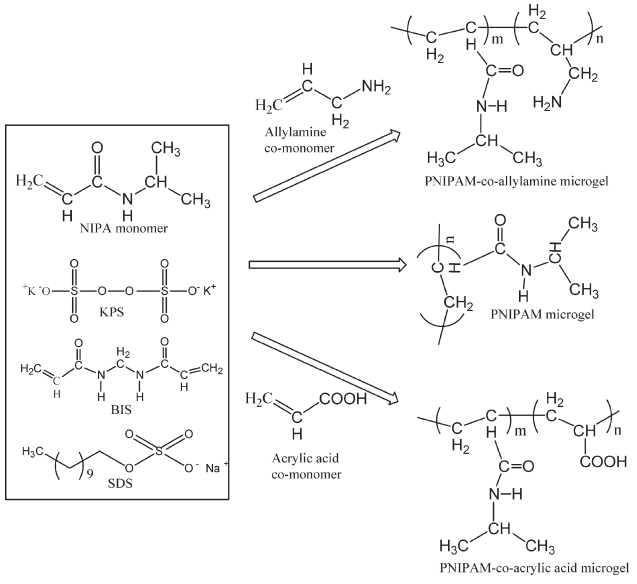

0.066 g of BIS, and 0.08 g of sodium dodecyl sulfate = "SDS" were dissolved in 245 g of distilled water. The solution was stirred under a nitrogen gas atmosphere for 40 min and then placed into a 60 °C hot bath. A 5.0 mL solution of potassium persulfate = "KPS" (0.166 g) was then added to initiate the radical polymerization. The reaction was continued for 5 h under a nitrogen atmosphere at 60 °C. The resultant PNIPAM-*co*-allylamine or PNIPAM-*co*-acrylic acid hydrogel colloidal particles were dialyzed against water for 1 week at room temperature and then further purified by ultracentrifugation.

2.4. Synthesis of Phosphorescent PNIPAM Microgels. Loading of the phosphor was carried out by stirring 10 mL of a 1.5 wt % aqueous solution of the relevant PNIPAM microgel and 3 mL of a 0.001 M aqueous solution of $Na_8[Au(TPPTS)_3]$ for 48 h under argon atmosphere, followed by centrifugation at 25 000 rpm for 3 h. After every 1 h of centrifugation the supernatant was discarded and the sediment washed with Millipore water. After three washes, the microgel obtained was incubated at around 22 °C for 2 days, allowing the formation of Au phosphor-loaded PNIPAM-*co*-allylamine or PNIPAM-*co*-acrylic acid microgel colloids or colloidal crystals.

2.5. Synthesis of Phosphorescent PNIPAM Hydrogel Networks. Crystalline luminescent microgels in water obtained after incubation were cross-linked using diglutaraldehyde as described elsewhere.[8c] Phosphorescent PNIPAM-*co*-allylamine crystalline microgel was added to diglutaraldehyde at neutral pH followed by incubation at 4 °C for chemical cross-linking. After 48 h, the fully cross-linked crystalline microgel network was removed and washed twice before storing in fresh Millipore water, resulting in formation of stable phosphorescent PNIPAM-*co*-allylamine engineered hydrogel crystal networks.

2.6. Formation of Lyophilized Hybrid Microgel. The dispersion of crystalline arrays of phosphorescent microgels was freeze-dried. After 7 days, the freeze-dried microgel was characterized by luminescence spectroscopy at room temperature and then redispersed in fresh Millipore water to check the loading stability of the gold phosphor. The redispersion was carried out by dipping the freeze-dried microgel into fresh Millipore water and then waiting for 24 h to check the photoluminescence stability of the redispersed phosphorescent gel.

2.7. Photoluminescence Characterization. All photoluminescence experiments were carried out with the PTI spectrofluorometer described below. For titrations, 2.5 mL aliquots were placed in the quartz cuvette (or 0.2 μL in a second experiment) and 0.1 mL of gel was added at every titration point with magnetic stirring. Titration data were plotted as I/I_0 vs volume of gel added (where I = intensity of sample after addition of gel and I_0 = intensity of pure aqueous gold phosphor solution). Lifetime data were analyzed using a xenon flash lamp or N_2 laser systems for both the sample and a scatterer solution used to generate the instrument response function (IRF) used for deconvolution.

2.8. Dynamic Light Scattering Characterization. The hydrodynamic radius of each sample was measured by dynamic light scattering (DLS). The details of the LLS instrumentation and theories have been described elsewhere.[8d] All measurements were done at a scattering angle of 90°. The temperature of the samples was controlled by a circulation water bath (Brinkmann Lauda Super RM-6) to within ±0.02 °C. The samples for all the dynamic light scattering analysis were prepared by homogenization followed by dilution with Millipore water. Each sample was measured three times, and the mean radius was reported. The zeta potential was measured on a zetasizer nano ZS (Malvern Instruments) loading samples into maintenance-free cells.

2.9. Spectroscopic Equipment. Steady-state luminescence spectra were acquired with a PTI QuantaMaster model QM-4 scanning spectrofluorometer equipped with a 75 W xenon lamp. The UV/vis absorption spectra were measured at 1 nm resolution on either a diode array spectrometer (Hewlett-Packard, model 8453) or a Perkin-Elmer Lambda-900 double-beam UV/vis/NIR absorption spectrophotometer.

2.10. UV−vis Spectroscopy Measurements. The turbidity (α) of the dispersions was measured vs wavelength using a UV−vis spectrophotometer by calculating the ratio of the transmitted (I_t) to incident (I_0) light intensity, $\alpha = -(1/d)\ln(I_t/I_0)$, where d is the thickness (1 cm) of the sampling cell.

3. Results

3.1. Spectroscopic Characterization of the Gold Phosphor. $Na_8[Au(TPPTS)_3]$ comprises a highly water-soluble three-coordinate Au(I) anionic complex that exhibits phosphorescence at room temperature in both aqueous solution and the solid state. According to the literature,[23] $Na_8[Au(TPPTS)_3]$ exhibits a broad emission band maximum at 494 nm in the solid state at room temperature, whereas at 77 K the emission intensity increases and undergoes a blue shift in peak maximum to 486 nm. In aqueous solution, the $[Au(TPPTS)_3]^{8-}$ emission is red-shifted with unsymmetrical broad emission band centering approximately at 515 nm. The absorption and photoluminescence spectra we obtained for the gold phosphor samples we synthesized were such that an aqueous solution of 0.001 M $[Au(TPPTS)_3]^{8-}$ exhibits a strong emission maximum at 525 nm and excitation maximum at 292 nm. The broad green emission band in solution is blue-shifted to turquoise blue in the solid state with unsymmetrical broad emission at 500 nm with excitation maximum at 356 nm. The photophysical properties observed for our samples synthesized are in overall good agreement with those reported by Assefa et al.[23] (see Supporting Information).

3.2. Luminescence Spectra of Different Hybrid Hydrogel Forms. The gold phosphor has been successfully loaded into three forms of PNIPAM-*co*-allylamine hydrogel systems: microgels in water, chemically cross-linked bulk hydrogel, and lyophilized freeze-dried xerogel. Figure 1 shows that these different forms of hydrogel systems after incorporating the gold phosphor exhibit similar photoluminescence spectra to those for the gold phosphor itself in aqueous solution or the solid state. This result suggests that the phosphor molecule retains its optical properties in its native form even in the presence of different hydrogel environments, which would be very attractive for different biological applications as most of the fluorescent dyes are expected to be sensitive to changes in microenvironment.[22b] Gold

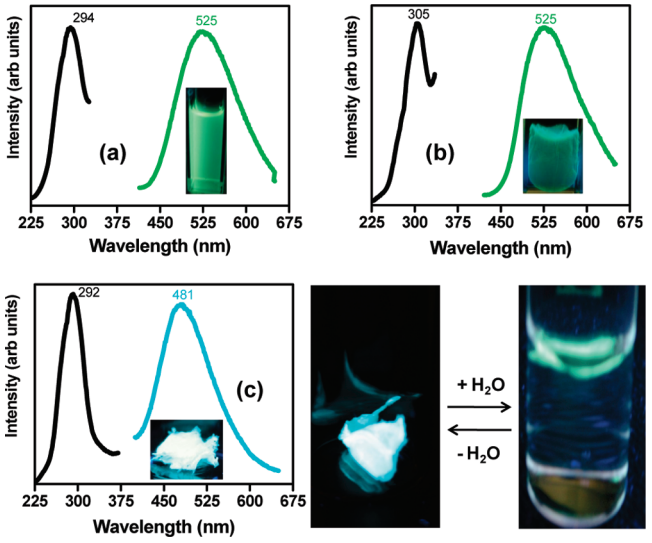

Figure 1. Photoluminescence spectra at room temperature for different forms of phosphorescent hydrogels: (a) microgels; (b) chemically cross-linked bulk hydrogel; (c) freeze-dried xerogel. This xerogel can be uniformly redispersed into water (bottom-right inset).

phosphor-loaded PNIPAM-*co*-allylamine microgel dispersion (Figure 1a) and the bulk hydrogel (Figure 1b) exhibit broad unsymmetrical green emission with λ_{max} near 525 nm, mirroring the emission of an aqueous solution of the phosphor. An increase in emission intensity accompanied by a blue shift to 490 nm is observed in the lyophilized freeze-dried xerogel (Figure 1c) at room temperature. The characteristic broad unsymmetrical emission bands from the gold phosphor are retained with minor shifts. Previous studies based on quantum mechanical computations illustrated the feasibility of systematic tuning of emission by controlling steric bulk in very similar three-coordinate Au(I) complexes, suggesting a Jahn−Teller distortion from a trigonal-planar ground state toward a T-shaped phosphorescent excited state.[24] PNIPAM microgels and bulk hydrogels in their swollen form in aqueous solution allow for a relatively unencumbered distortion toward the T-shaped geometry of the phosphorescent state, whereas the freeze-dried xerogel form entails a significant constraint to such a large molecular distortion. The underlying "luminescence rigidochromism" phenomenon in such three-coordinate d^{10} systems is addressed at a fundamental level elsewhere for water-insoluble complexes;[25] the phenomenon is well-known for other classes of phosphorescent molecules, including their use to monitor sol−gel−xerogel and other setting transformations in inorganic silicates.[26]

3.3. Influence of the Gold Phosphor on Inherent Hydrogel Properties. PNIPAM-*co*-allylamine microgels in water with polymer concentrations within 1.5−5.0 wt % can self-assemble into colloidal arrays with bright iridescent patterns at room temperature discussed elsewhere in detail.[8c] Even after loading the gold phosphor, hybrid microgels at a concentration of about 2.0 wt % self-assemble into a temperature sensitive ordered crystalline arrangement. Because of the Bragg diffraction from

(25) Sinha, P. Phosphorescent Emissions of Coinage Metal-Phosphine Complexes: Theory and Photophysics. Ph.D. Dissertation, Robert B. Toulouse School of Graduate Studies, University of North Texas, 2009.

(26) (a) Wrighton, M.; Morse, D. L. *J. Am. Chem. Soc.* **1974**, *96*, 998. (b) Fredericks, S. M.; Luong, J. C.; Wrighton, M. S. *J. Am. Chem. Soc.* **1979**, *101*, 7415. (c) Giordano, P. J.; Wrighton, M. S. *J. Am. Chem. Soc.* **1979**, *101*, 2888. (d) McKiernan, J.; Pouxviel, J. C.; Dunn, B.; Zink, J. I. *J. Phys. Chem.* **1989**, *93*, 2129. (e) Dunn, B.; Zink, J. I. *Chem. Mater.* **1997**, *9*, 2280. (f) Rickus, J. L.; Chang, P. L.; Tobin, A. L.; Zink, J. I.; Dunn, B. *J. Phys. Chem. B* **2004**, *108*, 9325. (g) Dunn, B.; Zink, J. I. *Acc. Chem. Res.* **2007**, *40*, 747. (h) Vogler, A.; Kunkley, H. *Mater. Chem. Phys.* **2008**, *109*, 506.

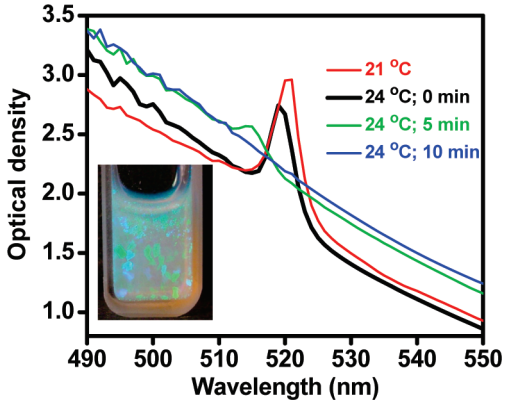

Figure 2. Turbidity vs wavelength for crystalline phosphorescent PNIPAM-*co*-allylamine microgel dispersions at two different temperatures. At 24 °C, both the peak height and peak wavelength decrease with time, indicating melting of crystalline structures.

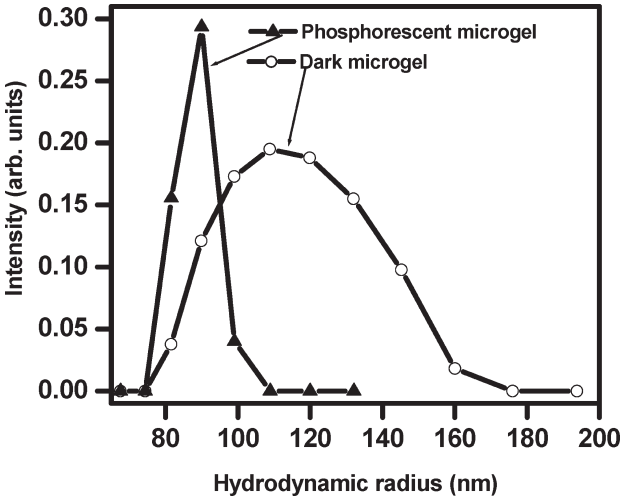

Figure 3. Dynamic light scattering data for PNIPAM-*co*-allylamine microgel before and after loading the gold phosphor.

the crystalline phase at 21 °C, the UV−vis spectrum exhibits a sharp attenuation peak (Figure 2), measured with UV−vis spectroscopy. At an elevated temperature (24 °C), both the peak height and peak wavelength decrease with time, indicating melting of crystalline structures. The shift in the sharp Bragg diffraction peak and its disappearance upon temperature increase in the hybrid phosphorescent microgels here is remarkably similar to the behavior with the unloaded PNIPAM microgel systems.[8e] This result signifies that the presence of gold phosphor does not result in sacrificing either formation or stimuli responsiveness of PNIPAM microgel crystals.

The magnitude of electrostatic attraction or repulsion is considered a key factor in controlling the dispersion mechanism of colloids in general. Loading the gold phosphor into PNIPAM-*co*-allylamine microgel dispersions due to electrostatic interactions in the aqueous medium is explained based on changes in dynamic light scattering data, zeta potential values, pH, and functional-group-dependent luminescence data obtained from various microgels studied at room temperature. Previous work by Frisken and co-workers[8b] illustrated a sharp decrease in particle size by introducing charged or ionic components into similar PNIPAM microgel systems. Figure 3 shows the hydrodynamic radius changes in PNIPAM-*co*-allylamine microgels after loading the gold phosphor, giving rise to a 23% decrease in R_h values, from 118 to 92 nm, under identical concentration

Scheme 2. Electrostatic Attraction That Leads to Size Reduction in the Phosphorescent Microgels of PNIPAM-*co*-Allylamine

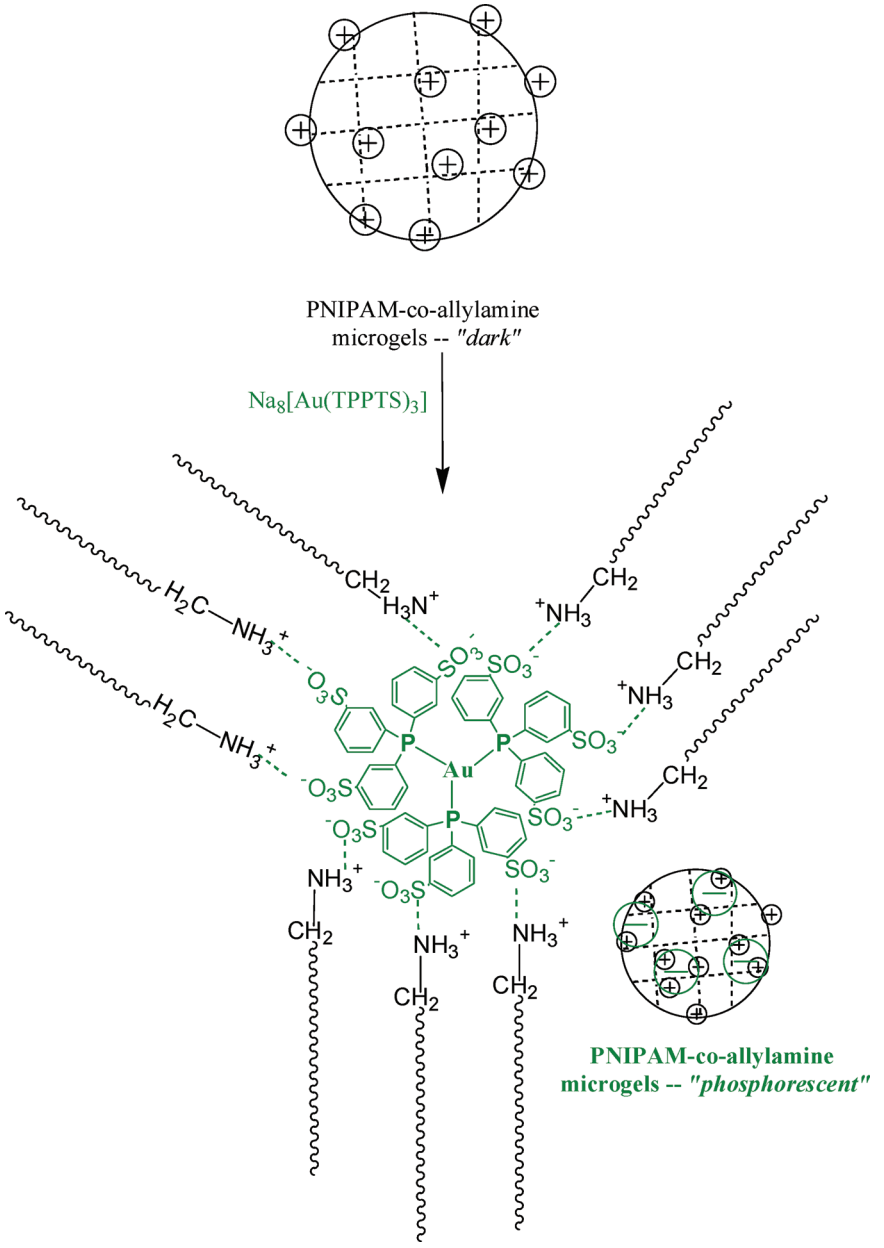

and experimental conditions. More impressively, the strong electrostatic interactions between the microgel particles and the gold phosphor also result in improved particle distribution, as clearly manifested by the remarkable reduction in the peak width of the DLS peak of the microgel dispersion after loading the gold phosphor by a factor of 4, from fwhm = 58 nm to 14 nm (Figure 3).

The changes in hydrodynamic radius emphasize charge component interactions between the gold phosphor and PNIPAM-*co*-allylamine microgel particles as observed elsewhere in similar microgel particles.[8b] Examination of zeta potential values also confirms the same conclusion. Thus, the +25.1 mV zeta potential value for the microgel at pH 5.0 before loading, which is attributed to positively charged protonated allylamine groups of microgel dispersion, decreases to +5.3 mV immediately after adding the gold phosphor . This decrease in zeta potential values in hybrid microgels clearly indicates adsorption of negatively charged phosphorescent complexes onto positively charged microgel spheres. On the basis of these results, we assume strong polyelectrolyte interactions between PNIPAM-*co*-allylamine microgel and the gold phosphor. Scheme 2 illustrates that the anionic Au(I) complex can effectively screen the interaction between positive charges on the micorgel and lead to size reduction of the microgel. It is noted that other factors may also contribute to the reduction of the particle size. For example, the diffusion coefficient is larger for charged colloids at lower ionic strengths, which corresponds to smaller size.[27]

The crystallinity of PNIPAM microgel crystals can be lost by shaking the dispersion at room temperature or heating the colloidal crystals just above room temperature. To stabilize the colloidal structure, the crystalline array of gold phosphor-loaded microgel particles were covalently cross-linked with diglutaraldehyde following a published procedure.[8c] The resulting hybrid bulk hydrogel network (Scheme 3) not only has a stable colloidal crystalline structure but also retains the broad green emission peak unchanged at 525 nm (Figure 1b). It is noted that the

(27) Doherty, P.; Benedek, G. B. *J. Chem. Phys.* **1974**, *61*, 5426.

Scheme 3. Formation of a Chemically-Cross-Linked Phosphorescent Hydrogel Network of PNIPAM-*co*-Allylamine[a]

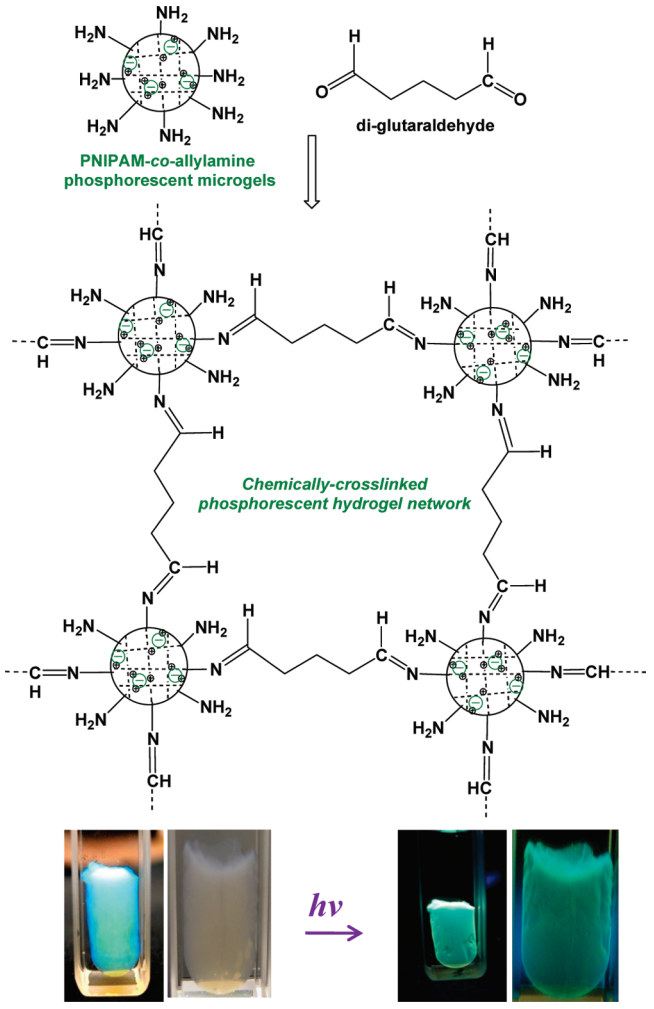

[a] The iridescent color of the crystalline product (or lack thereof to attain a colorless hydrogel network) can be controlled by varying the polymer concentration while the phosphorescence color remains the same, as illustrated.

fabrication of the hydrogel network form involves heating, slow cooling, followed by soaking the sample for 2 days in fresh Millipore water to remove excess unreacted diglutaraldehyde. If the gold phosphor were not well-entrapped within the matrix of the microgel, the so-formed network of microgel particles would not have retained any emission because the gold phosphor would have leached away during the process of soaking and water exchange. This suggests the presence of a strong electrostatic attraction between the PNIPAM-*co*-allylamine microgel and the gold phosphor. To our knowledge, this is the first example of a luminescent crystalline network that has been successfully obtained in aqueous medium.

Photoluminescence spectra recorded at room temperature for the lyophilized sample (Figure 1c) show a broad turquoise emission with maximum at 481 nm, similar to that for the gold phosphor solid. These spectra, however, are significantly different from those of the hybrid microgel aqueous samples with a significant blue shift. The lyophilized hybrid microgel can be redispersed into fresh Millipore water, regenerating the green emission characteristic of the aqueous microgel (Figure 1c, bottom-right inset). If $[Au(TPPTS)_3]^{8-}$ complexes were not strongly adsorbed or loaded into the freeze-dried form of the microgel, the heterogeneous physical mixture on redispersing into fresh Millipore water would have exhibited green emission uniformly from the entire aqueous solution. However, only the reswollen portion dispersed at the top exhibits green emission with no emission observed from the supernatant. These findings demonstrate stable loading of the gold phosphor into PNIPAM-*co*-allylamine microgels both in the solid and solution phase.

3.4. Functional Group and pH Dependence of Phosphor Loading. Guided by the steady-state photoluminescence data, loading of the gold phosphor into PNIPAM microgels is determined to depend on both the identity of the comonomer and the pH of the microgel solution. Loading studies were conducted for PNIPAM microgels with allylamine and acrylic acid comonomer functionalities at acidic and basic pH values. Figure 4 shows steady-state photoluminescence data for the gold phosphor loaded under these variations. The pH of the PNIPAM-*co*-allylamine microgel dispersion was adjusted from acidic values within 5.5−4.0 to basic values near 9.0 by addition of suitable volumes of 0.1 M acetic acid and 0.1 M ammonium hydroxide solutions, respectively, to the microgel dispersion. The efficiency of the gold phosphor loading can be readily determined by contrasting the photoluminescence intensity of supernatants vs sediments in each of the four samples studied. The most efficient loading is observed in PNIPAM-*co*-allylamine microgels at pH 4.0, whereas very little or no loading is observed in PNIAPM-*co*-acrylic acid microgels at pH 9.0 (see Supporting Information).

PNIPAM-*co*-allylamine microgels at pH 4.0 exhibit efficient loading of the gold phosphor. But for the same system at pH 9.0, the PL data indicate incomplete or inefficient loading. In the case of acrylic acid-based microgels at pH 9.0, on the other hand, all the gold phosphor was retained in the supernatant while the sediment did not exhibit any emission (Supporting Information), indicating 0% loading. At pH 4.0, the same acrylic acid microgel shows $<20\%$ emission intensity from the sediment of the microgel while most of the gold phosphor was still in the supernatant without being loaded. Among the four samples studied, only PNIPAM-*co*-allylamine microgels at acidic pH showed efficient loading of the Au phosphor, demonstrating the importance of pH and nature of the comonomer. Attachment of the gold phosphor to the surface of the microgel is, therefore, attributed to electrostatic interactions between the anionic sulfonate groups of the gold phosphor and the allylammonium groups of the comonomer in the PNIPAM-*co*-allylamine microgel. For the PNIPAM-*co*-acrylic acid microgel, the repulsive interaction between negatively charged gold phosphor and negatively charged carboxyl group in aqueous medium at pH 9.0 results in inefficient loading. The results also negate possible alternative mechanisms such as coordination of neutral amine groups from the PNIPAM-*co*-allylamine microgel or anionic carboxylate groups from the PNIPAM-*co*-acrylic acid microgel at basic pH. Both the stability of the three-coordinate geometry and softness of the Au(I) center are likely reasons for the insignificance of such possible coordination mechanisms. The strength of electrostatic interactions at different pH can be readily predicted based on pK_a values of different interacting functional moieties. The pK_a of allylamine and acrylic acid are 9.69 and 4.25, respectively, whereas the pK_a of benzenesulfonate is −6.5. Thus, one would predict that electrostatic interactions between the $-NH_3^+$ allylammonium groups amply dispersed at the surface of each microgel nanoparticle and the nine dissociated $-SO_3^-$ phenylsulfonate groups of each gold complex would result in efficient loading of the gold phosphor into the PNIPAM-*co*-allylamine microgel particles under both acidic and neutral pH. A previous report by Gong

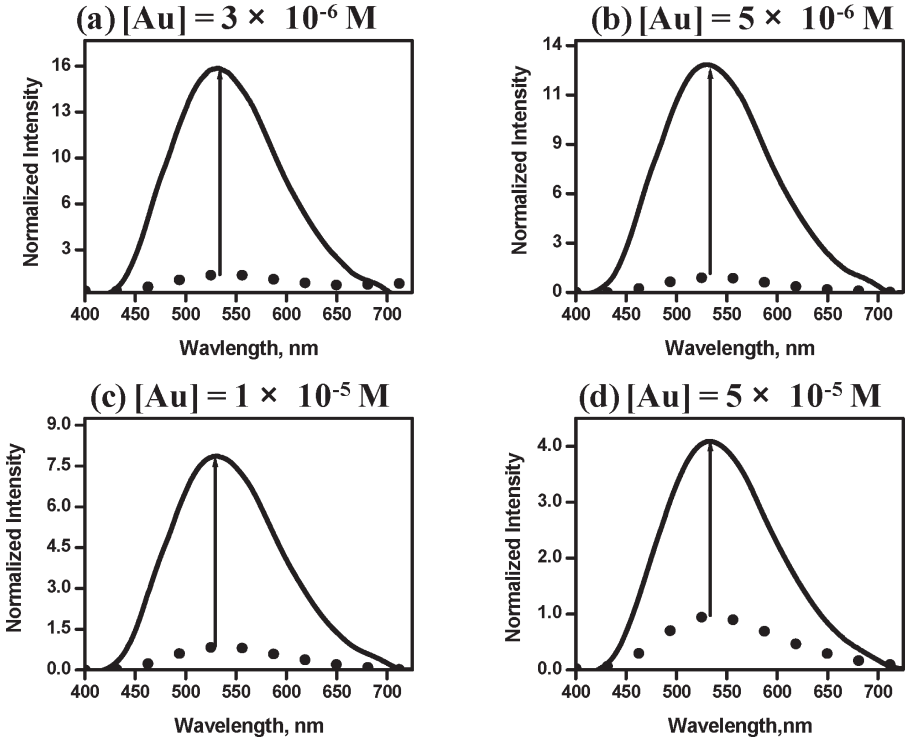

Figure 4. Photoluminescence enhancement in hybrid microgels at room temperature as a function of gold phosphor concentration. The spectra are shown before (dotted curves) and after (solid curves) addition of 0.1 mL of a 2% aqueous solution of PNIPAM-*co*-allylamine microgel to a 2.5 mL aqueous solution of the gold phosphor at pH 5.5.

et al. showed the entrapment of photoluminescent quantum dot (QD) nanocrystals into PNIPAM microspheres due to centrifugation force and weak hydrogen bonding between thioglycerol-capped CdTe nanocrystals and PNIPAM microspheres;[28] the stable fluorescent microspheres were observed after centrifugation only in the sediment compared to the supernatant of the sample. Uniform size of the nanocrystals and aggregation were controlling factors for loading such QD nanocrystals into PNIPAM microspheres. However, the present results suggest that such uniformity and aggregation problems can be avoided upon loading polyelectrolytic molecular phosphors like $Na_8[Au(TPPTS)_3]$ into PNIPAM microspheres.

3.5. Photoluminescence Enhancement. One can attain significant photoluminescence (PL) enhancement in multiple fashions upon incorporation of the gold phosphor in all hydrogel forms in this work. A dramatic manifestation is noticed upon titrating the gold phosphor with PNIPAM-*co*-allylamine microgels. The extent of PL enhancement can be varied by controlling the gold phosphor concentration, temperature above or below the volume phase transition temperature of the microgel, pH, etc. Titration experiments at various gold phosphor concentrations while keeping the concentration of the microgel constant are shown in Figure 4 while the effect of the microgel concentration is shown in Figure 5. The highest ratio of PL enhancement is attained at the lowest concentration of gold phosphor tested. In this set of experiments, we attain a 4-fold, 9-fold, 14-fold, 17-fold, and 50-fold PL enhancement upon decreasing the gold phosphor concentration along the direction 5×10^{-5}, 1×10^{-5}, 5×10^{-6}, 3×10^{-6}, and 1×10^{-6} M, respectively. Here we propose that, at a fixed microgel concentration, only a certain number of phosphorescent molecules will be loaded or are present in the vicinity of the microgel surface so as to contribute to the PL enhancement. The number of these molecules will not proportionally increase with an increase in concentration of the gold phosphor as concentration of microgel is fixed. So at higher concentration of gold phosphor molecules contributing to PL enhancement within the microgel will not increase compared to the number of phosphor molecules in the control or plain aqueous solution. This results in a decrease in the ratio of emission intensity enhancement at higher concentrations of the gold phosphor within the microgel environment, as shown. Titration experiments were also performed at basic (pH 9.0) conditions (Supporting Information); those attained smaller PL enhancement, as expected in view of the results of the previous section. The microgel concentration affects the PL enhancement in all the cases. For example, Figure 5 shows gradual PL enhancements up to 70-fold on addition of 0.2 mL of microgel while further microgel aliquots lead to slow decrease or a plateau; the inner-filter effect becomes relevant at higher gel concentrations.[29] A freshly synthesized sample of the Au phosphor was titrated with smaller quantities of microgel to diminish the inner-filter effect while amazingly increasing the PL enhancement up to 157-fold, essentially "*turning on*" the emission (Figure 5, bottom). These results signify that, at a fixed concentration of gold phosphor, the highest PL enhancement is attained at a critical concentration of microgel, which is very similar to the micellar effect on fluorescence enhancement as noticed by Takeuchi.[22e] The collection of experiments we performed suggests delicate interplay between the critical microgel concentration, concentration of the gold phosphor, pH, temperature, ionic strength, sample freshness, molecular weight, and refractive index of polymer gel, etc.—although we have not performed exhaustive

(28) Mohwald, H.; Wang, D.; Gao, M.; Gong, Y. *Chem. Mater.* **2005**, *17*, 2648.

(29) For representative examples, see: (a) MacDonald, B. C.; Lvin, S. J.; Patterson, H. *Anal. Chim. Acta* **1997**, *338*, 155. (b) Zhang, C.; Liu, M.-S.; Han, B.; Xing, X.-H. *Anal. Biochem.* **2009**, *390*, 197. For reviews, see: (c) Lloyd, J. B. F. *Tech. Vis. Ultraviol. Spectrom.* **1981**, *2*, 27. (d) Boens, N.; Ameloot, M.; Valeur, B. *Springer Ser. Fluoresc.* **2008**, *5*, 215.

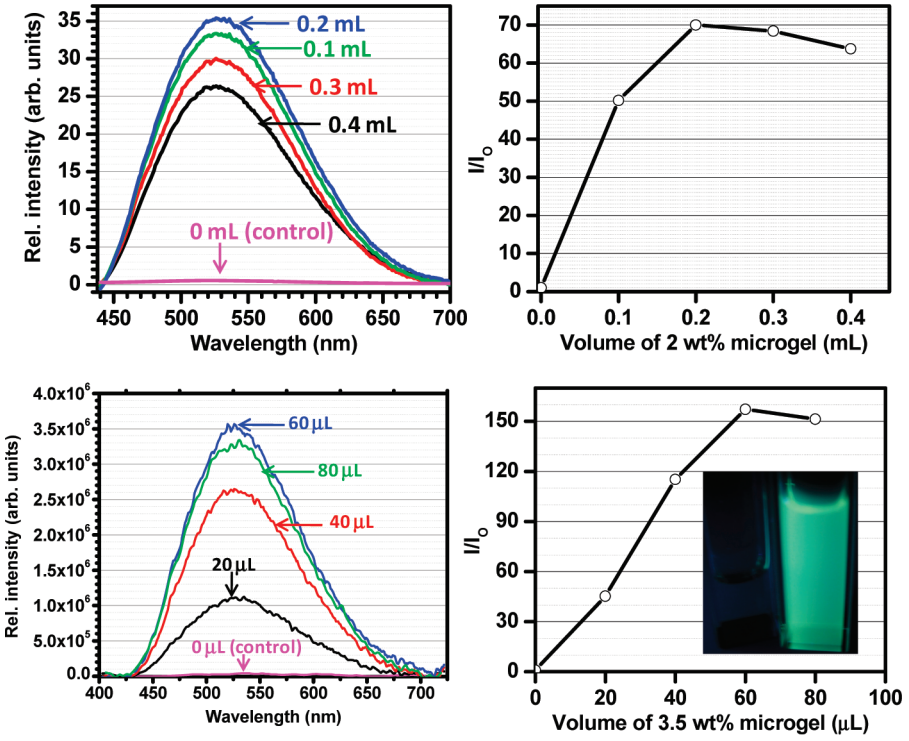

Figure 5. Photoluminescence enhancement of Au phosphor vs microgel concentration. The top panel shows results for a titration of an aqueous solution of ~1×10^{-6} M Au phosphor (2.50 mL) with 0.1 mL increments of ~2.0 wt % PNIPAM-*co*-allylamine microgel at pH 5.5 and room temperature. The bottom panel shows results of a similar titration for a 1×10^{-5} M sample of a freshly synthesized Au phosphor (3.00 mL) with 20 μL increments of ~3.5 wt % microgel. Neither sample was centrifuged to maximize phosphor entrapment in microgel spheres. The enhancement is plotted as I/I_0 with I and I_0 denoting the integrated emission peak area after and before adding the microgel, respectively, accounting for the dilution factor. The photograph illustrates the PL sensitization.

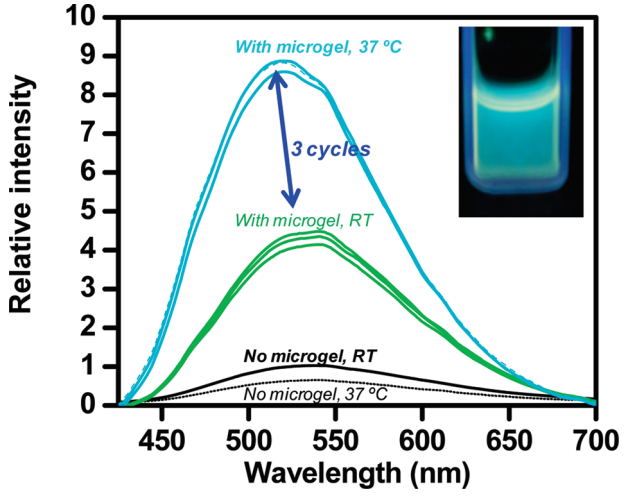

Figure 6. Temperature-dependent photoluminescence enhancement of the hybrid microgel upon heating from room temperature (RT) to 37 °C, contrasted with quenching for aqueous pure gold phosphor.

quantitative studies to maximize the relative or absolute PL enhancement under all these conditions.

An interesting situation is shown in Figure 6 in which a blue shift in emission maximum, from 532 to 515 nm, concomitant with emission enhancement, is seen upon heating microgels from ambient temperature to around 37 °C. The luminescence data in Figure 6 suggest that the physical state of heated hybrid microgel sample is intermediate between solution form and the lyophilized dried form. This result is consistent with the luminescence rigidochromism phenomenon discussed in section 3.2 for three-coordinate Au(I) complexes. Thus, the Jahn−Teller T-shaped distortion in the phosphorescent excited state from the trigonal ground-state geometry becomes more greatly hampered as one proceeds from the fluid solution, to the more viscous heated gel, and then to the lyophilized dried gel, leading to a greater blue shift in that direction. As shown in the temperature-dependent titrations in Figure 6, heating the gold phosphor microgel system to 37 °C results in not only a 620 cm^{-1} blue shift in emission maximum but also >100% PL enhancement, or more than doubling the emission intensity vs the gel at RT and a factor of 14 higher vs the aqueous solution without gel at 37 °C! This remarkable thermally induced PL enhancement is fully reversible, as shown by three heating/cooling cycles in Figure 6. The PL enhancement on heating is at least partially ascribed to the change of the microenvironment from hydrophilic to hydrophobic[8] as PNIPAM is heated above its lower critical solution temperature (LCST, which is about 34 °C). The PL enhancement is likely further assisted by an increase of the refractive index of the microgel when the temperatures is higher than the LCST, as observed previously in III−V semiconductor QD- or ZnO-embedded PNIPAM microgels.[30] The control study for an aqueous solution of the gold phosphor in absence of the PNIPAM microgel leads to quenching upon heating from ambient temperature to 37 °C, as expected due to increased nonradiative decay by multiphonon de-excitation to the ground state. This result is promising for possible utilization of the phosphprescent hybrid systems here for live bioimaging applications, for which a strong PL signal at the physiological temperature of 37 °C is critically important.

(30) (a) Neogi, A.; Garner, B.; Cai, T.; Kim, M.; Hu, Z. B. *Soft Mater.* **2009**, *7*, 232. (b) John, S.; Marpu, S.; Li, J.; Omary, M.; Hu, Z.; Fujita, Y.; Neogi, A. *J. Nanosci. Nanotechnol.* **2010**, *10*, 1707.

4. Discussion

The above findings are to be contrasted with other relevant studies in the literature. Photoluminescence was reported in lanthanide-doped hydrogel systems due to energy transfer from PNIPAM-*co*-styrene to Tb(III)[18b] or MMA:HEMA to Eu(III)[18c] phosphorescent centers, whereas the systems herein do not contain a chromophore in the hydrogel host and the transition-metal phosphorescent center contains chromophoric ligands already. The Eu(III)-doped MMA:HEMA hydrogel films exhibited pH-dependent photoluminescence due to populating the lanthanide excited state by sensitization, whereas here temperature and phosphor or hydrogel concentration also play major roles in the phosphorescence sensitization, in addition to pH. Notable literature precedents included the work of Li et al. in which a 4% PL enhancement was reported from different size quantum dots embedded in thermosensitive PNIPAM gels at room temperature.[21e] These authors attained nearly 10-fold quenching upon heating the PNIPAM/QD hybrid gels to near body temperature, unlike the dramatic enhancement we obtain in this work (Figure 6). Zhou and co-workers observed a 1.72-fold PL enhancement for terbium citrate upon binding to silver nanoparticles in solution, attributed to electric field enhancement around terbium from the electron plasmon resonance of silver nanoparticles.[22c] Takeuchi reported more significant PL enhancements of 8−20× for dansyl amino acid probes in presence of different surfactants due to micellar effects.[22e] The 1−2 order-of-magnitude PL enhancement seen herein in aqueous hydrogel media is rivaled only in purely organic media, which are usually less susceptible to quenching than aqueous media; e.g., a 40-fold PL enhancement for pyrene was reported upon embedding the fluorophore in hydrophobic polystyrene (toluene solution).[21b]

Phosphorescent transition metals have been incorporated in gel soft materials besides hydrogels, e.g., as described in the work of Dunn and Zink for Re(I) complexes in orthosilicate sol−gel systems,[26d−f] Aida and co-workers for Ag^+ adducts of trinuclear Au(I) complexes with 4-(3,5-dioctadecyloxybenzyl)-3,5-dimethylpyrazole organogels,[31] and Yam and co-workers for Pt(II) alkynyl complexes in 2,6-bis(*N*-dodecylbenzimidazol-2′-yl)pyridine.[32] We are also unaware of any precedents of hydrogel environments entrapping molecular or semiconductor species to exhibit photoluminescence in such a broad range of gel forms and/or responsiveness to the range of experimental variations that we report in this work.

As for the origin of PL sensitization, there are several mechanisms that have been invoked in prior literature precedents. Various groups reported that when a fluorophore is positioned within a restricted space provided by micelles or metallic nanoparticles, the electronic absorption and fluorescence spectra often change due to the effect of the microenvironment on fluorophores.[22] Increase in structural rigidity accompanied by decrease in accessibility to the surrounding aqueous medium in the presence of micelles decreases the nonradiative deactivation, resulting in fluorescence enhancement in fluorophores positioned within the microenvironment of micelles or vesicles.[22e,f] In the case of fluorophores localized close to metallic nanoparticles, fluorescence enhancement is explained as being due to intensified electromagnetic field from electronic plasmons, resulting in increased excitation rate or radiative rates.[22b] Finally, an increase in the refractive index of the microgel was invoked to explain PL enhancement in PNIPAM microgels embedded with III−V semiconductor quantum dots or ZnO nanoparticles.[29] These different explanations are all relevant to the PL enhancement observed herein. PNIPAM hydrogels indeed offer a micelle environment because they contain both hydrophilic and hydrophobic parts, thus limiting the quenching by water molecules compared to analogous aqueous solutions of the gold phosphor that do not contain the hydrogel. Both the electrostatic interactions (between the anionic gold complex and cationic ammonium groups of the hydrogel) and van der Waals or other hydrophobic interactions (between hydrocarbon and other nonpolar parts of the phosphor and PNIPAM moieties) act to reduce water quenching and thus the rate of nonradiative decay. In addition to the drastic PL enhancements seen in Figures 4−6, we have observed an increase of the phosphorescence lifetimes (from 1.4 to 2.6 μs in a typical example) for solutions that exhibit an order-of-magnitude PL intensity enhancement on addition of PNIPAM hydrogels to the aqueous solutions of the gold phosphor. The magnitude of the lifetime increase is less than the corresponding intensity increase, suggesting that suppressed nonradiative deactivation via multiphonon relaxation to the ground state is not solely responsible for the PL enhancement seen. Therefore, gel scattering must play at least some role in the PL sensitization, consistent with multiple literature precedents for other classes of emitters.[22f,33]

5. Conclusions

We report here stimuli-sensitive phosphorescent hydrogel microspheres synthesized by incorporating a transition-metal coordination compound, $Na_8[Au(TPPTS)_3]$, as phosphor into PNIPAM microgels. The resulting hybrid material exhibited sensitized Au-centered emission compared to that of the gold complex in water both above and below the volume phase transition temperature of the microgel. The resulting phosphorescent microspheres showed decreased size and PL enhancement with particularly high phosphorescence sensitization at physiological pH and temperature. The results show strong dependency of the phosphor loading on pH and nature of functional group to maximize the interactions between the PNIPAM microgel host and the gold phosphor guest. These results encourage us to develop new classes of water-soluble transition-metal complexes which can serve multiple functions to act as phosphorescent physical cross-linkers of various biopolymers, biological labeling reagents for imaging, and/or optical sensors for various biological and environmental applications (Patent Pending).

Acknowledgment. The authors gratefully acknowledge financial support from the National Science Foundation (Grants CHE-0349313 to M.A.O. and DMR-0805089 to Z.H.) and the Robert A. Welch Foundation (Grant B-1542 to M.A.O.).

Supporting Information Available: Further spectroscopic data and analysis details referred to in the text. This material is available free of charge via the Internet at http://pubs.acs.org.

Note Added after ASAP Publication. This article was published ASAP on September 13, 2010. Scheme 1 has been modified. The correct version was published on September 28, 2010.

(31) Kishimura, A.; Yamashita, T.; Aida, T. *J. Am. Chem. Soc.* **2005**, *127*, 179.
(32) Tam, A. Y.-Y.; Wong, K. M.-C.; Yam, V. W.-W. *J. Am. Chem. Soc.* **2009**, *131*, 6253.
(33) (a) Lawandy, N. M.; Balachandran, R. M.; Gomes, A. S. L.; Sauvain, E. *Nature* **1994**, *368*, 436. (b) Tam, F.; Goodrich, G. P.; Johnson, B. R.; Halas, N. J. *Nano Lett.* **2007**, *7*, 496.